Journal of the European Ceramic Society **9** (1992) 53–60

The Reaction of AlN with some Metal Oxides at High Temperatures

P. Cannard,[a]* Thommy Ekström[b] & R. J. D. Tilley[a]‡

[a] Division of Materials, School of Engineering, University of Wales College of Cardiff, P.O. Box 917, Cardiff CF2 1XH, UK

[b] Department of Inorganic Chemistry, Arrhenius Laboratory, University of Stockholm, S-10691 Stockholm, Sweden

(Received 4 March 1991; revised version received 3 May 1991; accepted 10 May 1991)

Abstract

The reaction between AlN and small amounts of the oxides MgO, TiO_2, Cr_2O_3, Fe_2O_3, Y_2O_3, ZrO_2, Nb_2O_5 or Ta_2O_5 has been studied at temperatures of 1820°C and 1950°C. All reactants were embedded in BN powder and heated in a graphite furnace under a nitrogen atmosphere. At 1820°C MgO, TiO_2, Cr_2O_3, Fe_2O_3, Nb_2O_5 and Ta_2O_5 reacted to form the non-stoichiometric oxynitride spinel phase $\approx Al_{23}O_{27}N_5$ and Mg_3N_2, Ti(C,N), CrB, Fe_2B, NbC or TaC. At 1950°C aluminium oxynitride polytypoids were formed in place of the spinel. These possessed a needle-like morphology in the AlN–MgO, AlN–TiO_2 and AlN–Cr_2O_3 systems and an equiaxed morphology in the AlN–Fe_2O_3 and AlN–Nb_2O_5 systems. The AlN–ZrO_2 samples reacted to form only Zr(C,N) and the AlN–Y_2O_3 samples reacted to form only $Al_2Y_4O_9$.

Die Reaktion von AlN mit geringen Anteilen an MgO, TiO_2, Cr_2O_3, Fe_2O_3, Y_2O_3, ZrO_2, Nb_2O_5 und Ta_2O_5 wurde bei 1820°C und 1950°C untersucht. Alle Mischungen wurden in BN-Pulver eingebettet und im Kohlewiderstandsofen unter Stickstoffatmosphäre getempert. Bei 1820°C reagierten MgO, TiO_2, Cr_2O_3, Fe_2O_3, Nb_2O_5 und Ta_2O_5 zur nichtstöchiometrischen Oxinitridspinellphase $\approx Al_{23}O_{27}N_5$ und Mg_3N_2, Ti(C,N), CrB, Fe_2B, NbC oder TaC. Bei 1950°C bildeten sich anstatt der Spinellphase Aluminiumoxinitridpolytypen. Diese wiesen im AlN–MgO-, AlN–TiO_2- und AlN–Cr_2O_3-System eine nadelförmige Morphologie auf, im AlN–Fe_2O_3- und AlN–Nb_2O_5-System dagegen eine globulare Morphologie. Die AlN–ZrO_2-Proben bildeten nur Zr(C,N) und die AlN–Y_2O_3-Proben nur $Al_2Y_4O_9$.

On a étudié la réaction entre AlN et de faibles quantités des oxydes MgO, TiO_2, Cr_2O_3, Fe_2O_3, Y_2O_3, ZrO_2, Nb_2O_5 et Ta_2O_5 à des températures de 1820 et 1950°C. Tous les réactifs étaient placés dans un lit de poudre de BN et chauffés dans un four graphite sous atmosphère d'azote. A 1820°C MgO, TiO_2, Cr_2O_3, Fe_2O_3, Nb_2O_5 et Ta_2O_5 réagissaient pour former une phase spinelle d'oxynitrure non stoechiométrique $\approx Al_{23}O_{27}N_5$ et Mg_3N_2, Ti(C,N), CrB, Fe_2B, NbC et TaC. A 1950°C des polytypes d'oxynitrure d'aluminium se formaient à la place de la phase spinelle. Ceux-ci présentaient une morphologie aciculaire dans les systèmes AlN–MgO, AlN–TiO_2 et AlN–Cr_2O_3 et une morphologie équiaxe dans les systèmes AlN–Fe_2O_3 et AlN–Nb_2O_5. Les échantillons AlN–ZrO_2 conduisaient à la formation de Zr(C,N) seul et les échantillons AlN–Y_2O_3 à la formation de $Al_2Y_4O_9$ seul.

1 Introduction

The compound AlN has a number of interesting physical properties that make it a candidate for a variety of electronic and structural engineering applications.[1] However, it suffers from the usual mechanical and structural problems associated with strongly covalent ceramic materials. Traditionally these problems are often overcome by reacting the primary material with small amounts of other compounds which may, for example, enhance sintering or eliminate gross structural defects. These aspects are reviewed by Virkar *et al.*[1] As part of a programme aimed at the production of improved ceramics, the present authors have studied the

* Present address: G.35/B55 (RT2315), British Telecom Research Laboratories, Martlesham Heath, Ipswich IP5 7RE, UK.
‡ To whom correspondence should be addressed.

Journal of the European Ceramic Society 0955-2219/92/$5.00

compounds formed when AlN reacts at high temperatures with small amounts of a variety of other oxides in a graphite furnace.

The reactant oxides investigated were MgO, TiO_2, Cr_2O_3, Fe_2O_3, Y_2O_3, ZrO_2, Nb_2O_5 and Ta_2O_5. No research has been reported on the Fe_2O_3–AlN, Nb_2O_5–AlN or Ta_2O_5–AlN systems. The phases obtained when AlN reacts with the other compounds at high temperatures have been reported mainly in the context of sinterability or densification.[2-10] The results obtained in this study show that reaction with the furnace surroundings predominates and the ternary metals used in the study seem not to form compounds with AlN under the experimental conditions employed. However, they do influence the microstructures of the AlN polytypoid phases formed, a finding of relevance to the strengthening of multiphase ceramic components.

2 Experimental

Samples were prepared from high purity reagents supplied by Johnson-Matthey. The AlN was stored in an evacuated desiccator to prevent reaction with water vapour which produces a surface layer of Al_2O_3 on the AlN grains. 5:1, 10:1, 20:1 and 50:1 molar ratios of AlN–MgO, AlN–TiO_2, AlN–Cr_2O_3, AlN–Fe_2O_3, AlN–Y_2O_3, AlN–ZrO_2, AlN–Nb_2O_5 and AlN–Ta_2O_5 were each mixed in an agate mortar before being pressed into 13-mm diameter pellets. The pellets were heated in two different types of container. In the first case, pellets were placed in graphite trays. In order to reduce carbon contamination, the trays were coated with BN and the samples surrounded by additional layers of powdered BN. If sample volatility was suspected the pellets were placed inside a solid BN crucible, packed with powdered BN and sealed with a tight-fitting BN lid in order to reduce the loss of metal oxide. A graphite-lined furnace with graphite heating elements and a controlled atmosphere capability was used to heat the samples at 1820°C or 1950°C. Details of the heating cycles are given in Table 1. The complex heating sequence was designed to remove all pressing aids and to prevent cracking of the samples. The temperature within the furnace was monitored automatically with thermocouples and manually using an optical pyrometer.

Powder X-ray diffraction was carried out using IRD XDC 700 and IRD XDC 1000 Hägg–Guinier focusing cameras employing strictly monochromatic Cu$K_{\alpha 1}$ radiation and KCl ($a_0 = 0{\cdot}629\,23$ nm at 25°C) as an internal standard. The films were measured using a scale graduated in 0·1 mm intervals exposed on the film prior to development. Unit cell data were obtained from the line positions using standard computer routines.[11]

Table 1. Heating cycles for 1820°C and 1950°C preparations

Temperature (°C)	*Time (h)*	*Atmosphere*
20–200	0·5	Vacuum
200–500	1·6	Vacuum
500	0·2	Vacuum
500–700	0·6	1 atm N_2
700–1100	0·6	1 atm N_2
1100–1400	0·5	1 atm N_2
1400–1750	0·5	1 atm N_2
1750–1820	0·2	1 atm N_2
1820	5·0	1 atm N_2
20–200	0·5	Vacuum
200–500	1·6	Vacuum
500	0·2	Vacuum
500–1820	2·25	1 atm N_2
1820–1950	1·1	1 atm N_2
1950	1·0	1 atm N_2

For morphology studies pellets were fractured to reveal fresh internal surfaces which were examined in a JEOL JEM 35CF scanning electron microscope equipped with energy and wavelength dispersive analysis systems and operated at 21 kV. The fracture surfaces were carbon coated before examination to prevent charging.

Samples for transmission electron microscopy were prepared by crushing a small amount of material under *n*-butanol in an agate mortar. A drop of the resulting suspension was allowed to dry on a copper grid previously covered with a holey carbon film before examination in a JEOL 200CX transmission electron microscope fitted with a high resolution top entry goniometer stage and operated at 200 kV.

3 Results

3.1 1820°C Sintering cycle

3.1.1 X-ray diffraction

These results are presented in Table 2 and summarised in Fig. 1(a). The non-stoichiometric spinel phase $\approx Al_{23}O_{27}N_5$ formed in all systems except Y_2O_3–AlN and ZrO_2–AlN. In the MgO–AlN system this was the only phase found, although it is presumed that Mg_3N_2 was also formed and was lost by volatilisation.[5] In the other systems the additional phase was a carbide, NbC or TaC, a carbonitride, Ti(C, N) or Zr(C, N), or a boride, CrB, Fe_2B or TaB. The Ti(C, N) phase had a cubic unit cell with $a_0 = 0{\cdot}426\,46 \pm 0{\cdot}000\,08$ nm. Using powder

Table 2. X-Ray diffraction phase analysis

Starting ratios	*Phases present*[a]	
	1820°C	*1950°C*
AlN:MgO		
5:1	((AlON))	AlN, 27R
10:1	AlN	(27R), ((C))
20:1	AlN	((27R)), ((C))
50:1	AlN	(C)
$AlN:TiO_2$		
5:1	Ti(C, N), (AlON)	Ti(C, N), (27R)
10:1	Ti(C, N), AlON	Ti(C, N), ((27R))
20:1	Ti(C, N)	(Ti(C,N))
50:1	Ti(C, N)	AlN
$AlN:Cr_2O_3$		
5:1	(AlON), (CrB), (A)	
10:1	(CrB), ((A))	21R, (CrB), (D)
20:1	AlN	27R, (CrB)
50:1	AlN	((27R)), ((CrB))
$AlN:Fe_2O_3$		
5:1	AlON, Fe_2B	21R, Fe_2B, (AlON) ((27R)), ((E))
10:1	AlON, Fe_2B	27R, Fe_2B, (E)
20:1	(Fe_2B)	(27R), (E)
50:1	((Fe_2B))	(27R), (E)
$AlN:Y_2O_3$		
5:1	Y_2O_3, ($Y_4Al_2O_9$)	Y_2O_3
10:1	Y_2O_3, ($Y_4Al_2O_9$)	Y_2O_3, ($Al_2Y_4O_9$)
20:1	Y_2O_3, (($Y_4Al_2O_9$))	(Y_2O_3), ($Al_2Y_4O_9$)
50:1	Y_2O_3, (($Y_4Al_2O_9$))	(Y_2O_3), ($Al_2Y_4O_9$)
$AlN:ZrO_2$		
5:1	Zr(C, N)	Zr(C, N)
10:1	Zr(C, N)	Zr(C, N)
20:1	((Zr(C, N)))	Zr(C, N)
50:1	((Zr(C, N)))	Zr(C, N)
$AlN:Nb_2O_5$		
5:1	Not recovered	F, 21R, NbC, (G), (AlON)
10:1	AlON, NbC, (B)	21R, F, NbC, (G), (27R)
20:1	Not recovered	27R, NbC, F, (G)
50:1	NbC, (AlON), ((B))	NbC, F, (AlON), (G)
$AlN:Ta_2O_5$		
5:1	TaC, AlON, (TaB)	TaC
10:1	TaC, (AlON), (TaB)	TaC
20:1	TaC, (AlON)	TaC
50:1	TaC	TaC

[a] All samples contained the starting material AlN, which has been omitted from the table except where it was the only phase found. Unidentified phases are denoted by the letters A–G. The phases are listed in order of diminishing quantity; those present in only small or trace amounts are surrounded by parentheses or double parentheses respectively. AlON represents the non-stoichiometric spinel phase, $\approx Al_{23}O_{27}N_5$.

diffraction data for TiN and TiC,[12] and assuming Vegard's Law holds, the approximate composition of the Ti(C, N) phase produced here was $TiC_{0.3}N_{0.7}$. The Zr(C, N) had a cubic unit cell with $a_0 = 0{\cdot}463\,92 \pm 0{\cdot}000\,06$ nm. A similar approach using powder diffraction data for ZrN and ZrC[13] suggested that the Zr(C, N) phase in this study has a

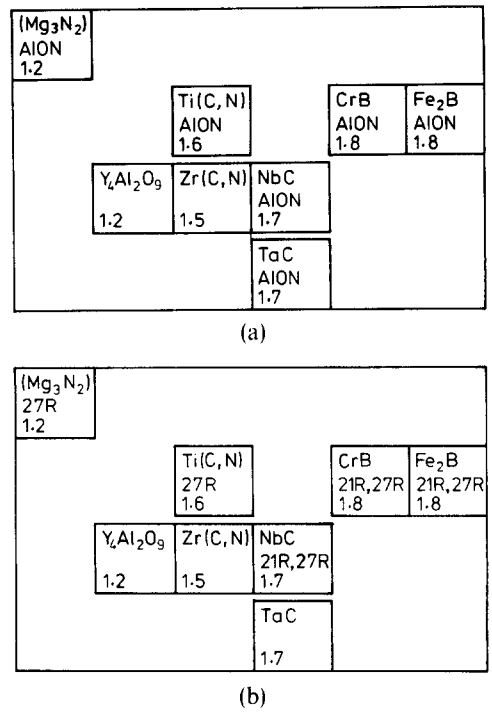

Fig. 1. The principle phases formed in the AlN–M_aO_b systems at (a) 1820°C and (b) 1950°C set out in the form of an abbreviated periodic table. Mg_3N_2 was not observed and is presumed to have vaporised. AlON refers to the non-stoichiometric spinel phase $\approx Al_{23}O_{27}N_5$. The numerical values are electronegativities of the elements, taken from Ref. 14.

composition of approximately $ZrC_{0.5}N_{0.5}$. In the Y_2O_3–AlN system $Y_4Al_2O_9$ was the only phase formed.

3.1.2 Scanning electron microscopy

Two samples were studied by scanning electron microscopy, $5AlN:1Cr_2O_3$ and $5AlN:1Fe_2O_3$. The general morphology of both samples was similar and consisted mainly of equiaxed grains together with some easily distinguished larger grains, shown in Fig. 2. EDAX analysis of the equiaxed grains indicated only the presence of Al, leading to the conclusion that this material is AlN or the non-stoichiometric spinel $\approx Al_{23}O_{27}N_5$. EDAX analysis of the larger crystals showed only Cr or Fe peaks, and reference to the X-ray diffraction analysis revealed that these were CrB or Fe_2B. Spot analysis on a large number of particles indicated that there appeared to be no dissolution of Al into the borides, or Cr or Fe into the AlN or $\approx Al_{23}O_{27}N_5$ grains. A few very fine needles, of dimensions less than $0{\cdot}5\,\mu m \times 5\,\mu m$, which were not possible to identify, were also observed in the $5AlN:1Fe_2O_3$ sample.

3.2 1950°C Sintering cycle

3.2.1 X-ray diffraction

These results, presented in Table 2 and summarised in Fig. 1(b), were rather similar to those at the lower

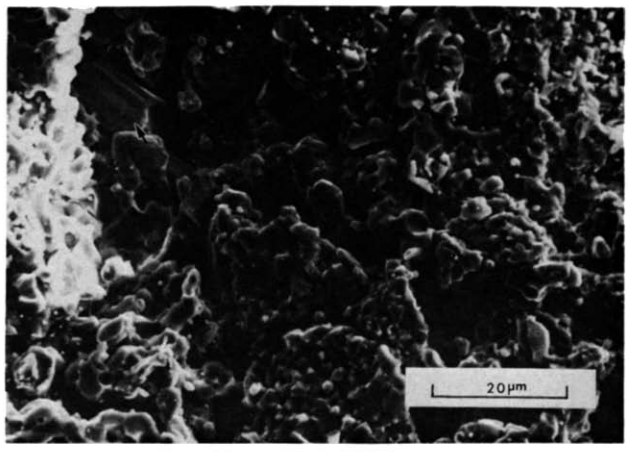

(a)

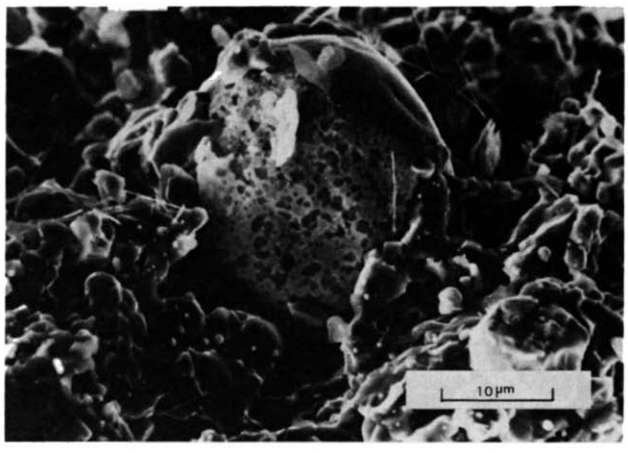

(b)

Fig. 2. (a) Scanning electron micrograph of the fracture surface of the 1820°C 5AlN:1Cr_2O_3 sample consisting mainly of angular equiaxed grains which are probably AlN or an oxynitride spinel. A grain of quite different morphology (arrowed) contains only Cr and is probably CrB. (b) Scanning electron micrograph of the fracture surface of the 1820°C 5AlN:1Fe_2O_3 sample. This reveals a smooth round grain with a mottled surface, probably Fe_2B.

reaction temperature. There are two principal differences, the non-stoichiometric spinel phase $\approx Al_{23}O_{27}N_5$ was replaced by 27R or 21R AlN polytypoids and a number of new and unidentified phases formed. The Ti(C, N) phase had a cubic unit cell with $a_0 = 0{\cdot}426\,46 \pm 0{\cdot}000\,08$ nm and an approximate composition of $TiC_{0{\cdot}3}N_{0{\cdot}7}$,[12] unchanged from that at lower temperatures. The Zr(C, N) had a cubic unit cell with $a_0 = 0{\cdot}465\,64 \pm 0{\cdot}000\,04$ nm, indicating that the composition was approximately $ZrC_{0{\cdot}7}N_{0{\cdot}3}$,[13] i.e. slightly carbon-rich compared to that at the lower temperature.

3.2.2 Scanning electron microscopy

The morphologies of these preparations fell into four groups, as follows.

(i) The 5AlN:1MgO, 5AlN:1TiO_2 and 10AlN:1Cr_2O_3 samples were all similar and consisted of a mixture of needle-like and equiaxed grains, identified respectively as AlN polytypoids and AlN. Figure 3 shows an example taken from the 10AlN:1Cr_2O_3 preparation. EDAX analysis of both the needles and the equiaxed grains revealed the presence of only Al and no other metal. The ternary metal was found as isolated crystals of Ti(C, N) and CrB, except for the 5AlN–MgO sample where Mg was not encountered due to the volatilisation of Mg_3N_2.[5] The morphology of the Ti(C, N), clusters of small particles, is shown in Fig. 4. The morphology of the CrB was identical to that occurring at 1820°C.

(ii) The morphology of the 5AlN:1Fe_2O_3 sample is shown in Fig. 5, which reveals two features, a granular texture which extended over the entire face of the specimen and several faceted crystals seen towards the

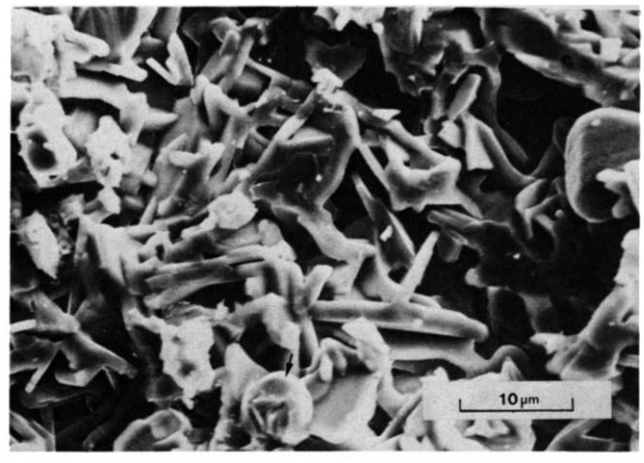

Fig. 3. Scanning electron micrograph of the fracture surface of the 1950°C 10AlN:1Cr_2O_3 sample. The needles contain only Al as the metallic component. Arrowed is a Cr-containing grain which is likely to be CrB.

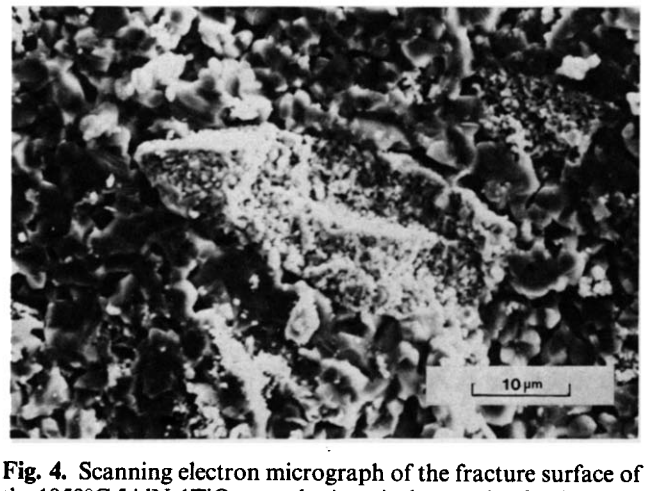

Fig. 4. Scanning electron micrograph of the fracture surface of the 1950°C 5AlN:1TiO_2 sample. A typical example of a cluster of Ti-containing grains, as found throughout this sample, is shown.

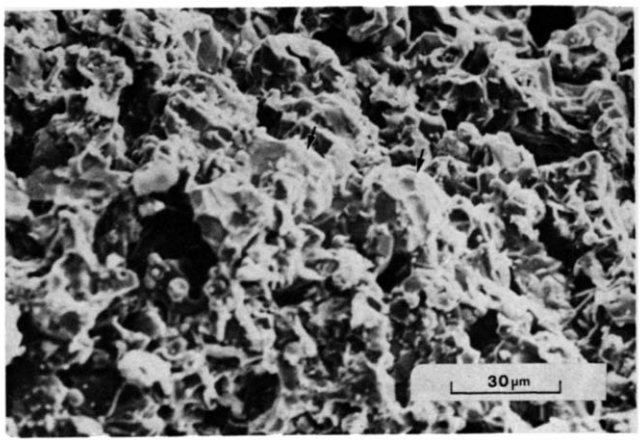

Fig. 5. Scanning electron micrograph of the fracture surface of the 1950°C 5AlN:1Fe_2O_3 sample. The texture appears granular with porosity visible. No needle-like AlN polytype grains were observed. Towards the centre of the figure are several crystals (arrowed) which were probably Fe_2B.

centre of the figure. EDAX analysis suggested that these latter particles were probably Fe_2B. The 5AlN:1Nb_2O_5 sample examined was similar in morphology, but less coarse, to that shown in Fig. 5. Additionally this sample contained small rounded grains varying in size from less than 1 μm to several μm in diameter similar to those shown in Fig. 4. EDAX analysis showed this phase to be NbC or one of the unknown phases found in this system.

(iii) Figure 6 shows the microstructure of the 5AlN:1Y_2O_3 sample. It is composed of interlocking plates with small, more equiaxed grains lying between them. An EDAX analysis of these plates showed that some only contained Y, while others contained approximately equal amounts of Al and Y, leading to the conclusions that the respective phases were Y_2O_3 and $Al_2Y_4O_9$.

(iv) The 50AlN:1Y_2O_3 microstructure shown in Fig. 7 consisted of round, equiaxed grains surrounded by a thin layer of a different material. EDAX analysis revealed that the thin layer was $Al_2Y_4O_9$ and the rounded grains were probably AlN.

3.2.3 Transmission electron microscopy of polytypoids

The transmission electron microscope analysis, which concentrated on the polytypoids encountered in this study, is given in Table 3. Most of the crystal fragments examined were well ordered and corresponded to the structures 33R, 27R and 21R. An image of a well-ordered 21R phase found in

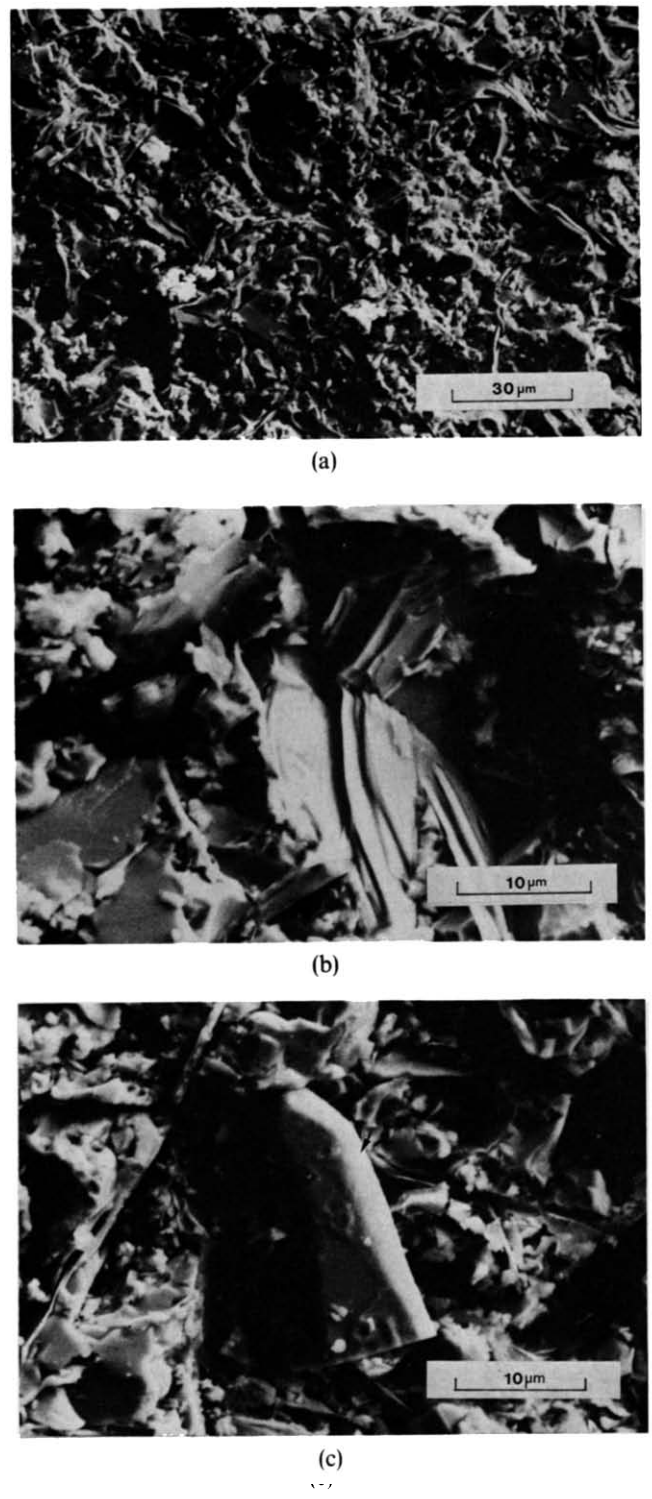

Fig. 6. (a) Scanning electron micrograph of the fracture surface of the 1950°C 5AlN:1Y_2O_3 sample showing a surface almost devoid of porosity. (b) An enlarged view of a plate-like microstructure. EDAX analysis revealed these plates to contain only Y. (c) A grain (arrowed) containing approximately equal proportions of Al and Y.

5AlN:1Fe_2O_3 is shown in Fig. 8. The disorder found in these crystals usually took the form of slabs of different thicknesses coherently intergrown in the crystal matrix. As an example Fig. 9 shows a disordered fragment from a sample of overall

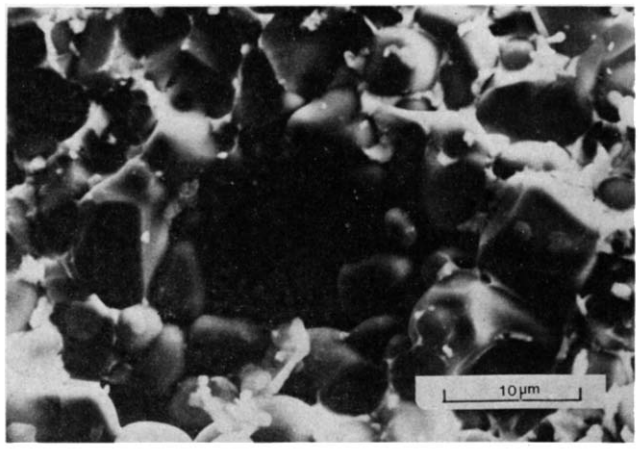

Fig. 7. Scanning electron micrograph of the fracture surface of the 1950°C 50AlN:1Y_2O_3 sample. The rounded grains could be identified as AlN. EDAX analysis of the honeycomb surround revealed it to contain Al and Y.

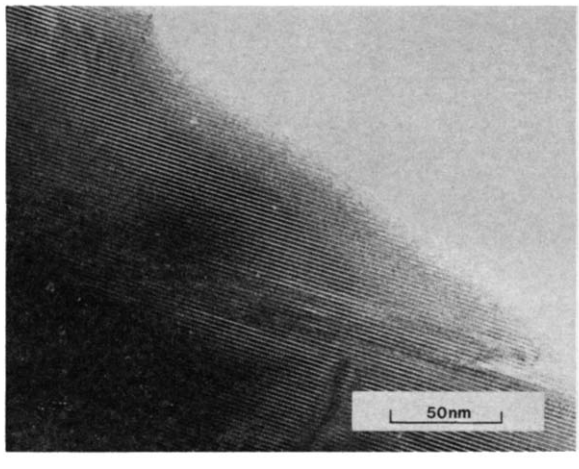

Fig. 8. Electron micrograph of a fragment of a well-ordered 21R AlN polytype taken from the 5AlN:1Fe_2O_3 sample.

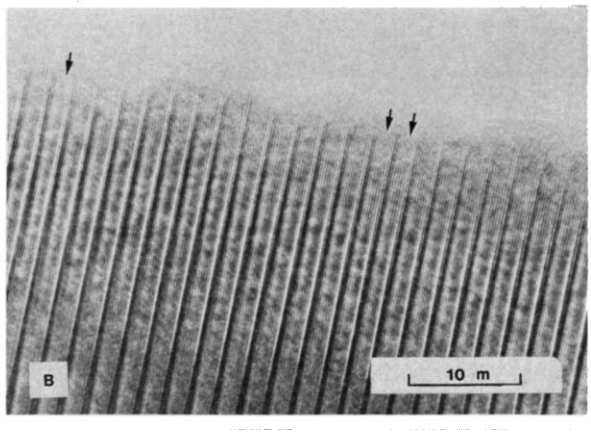

Fig. 9. Electron micrograph of a polytype fragment taken from the 10AlN:1Fe_2O_3 sample containing irregularly placed slabs of eight and nine metal layers (arrowed).

Table 3. Transmission electron microscope phase analysis of polytypoid crystals

Sample	*21R*	*16H*	*27R*	*33R*	*Disordered*	*Total*
10AlN:1MgO	—	—	1	3	1	5
5AlN:1TiO_2	—	—	3	—	—	3
10AlN:1Cr_2O_3	6	1	1	—	2	10
5AlN:1Fe_2O_3	4	—	1	—	—	5
10AlN:1Fe_2O_3	—	—	3	—	3	6
20AlN:1Fe_2O_3	—	—	3	—	—	3
50AlN:1Fe_2O_3	—	—	3	1	—	4
5AlN:1Nb_2O_5	3	—	—	—	—	3
10AlN:1Nb_2O_5	—	—	3	—	—	3

composition 10AlN:1Fe_2O_3. The crystal is 27R polytypoid containing coherently intergrown whole or half blocks of the 16H polytypoid.

4 Discussion

The results presented show that the metal oxides employed in this study, with the exception of Y_2O_3, reacted to form nitrides, carbides, carbonitrides or borides, although in the case of MgO, no nitride was observed, in agreement with the findings of Jack,[5] who reported that Mg_3N_2 was lost by volatilisation at high temperatures. The volatility problem may also account for the fact that the known MgAlON spinel phase[5] was also not observed in this study. The oxygen liberated in the reactions combined with AlN to form the non-stoichiometric spinel $\approx Al_{23}O_{27}N_5$ at 1820°C and AlN polytypoids at 1950°C. Thus, within the accuracy of the analytical equipment, none of the added metal entered these oxynitride phases and a complete segregation took place. This is somewhat surprising in the case of Cr and Fe, as these metals can replace Al in Al_2O_3 and some incorporation of these ions into the spinel phase might be expected. Similarly the wurtzite structure is well represented in nature and cation substitution is well known. It therefore seems that although such substitutions are possible in theory they do not take place in practice. This might reflect the very high stability of the other phases under the preparations employed in this study. The Y_2O_3–AlN system behaved in a different fashion to the others as the oxygen remained bound to the Y via the phases Y_2O_3 and $Y_4Al_2O_9$. These findings are in agreement with previous studies.[2,3]

There appears to be a clearly defined periodic trend in the reaction products formed, which is displayed in Fig. 1. The element nearest the top left of the 'periodic table' (Mg), we presume to have formed a nitride. As one moves towards the lower right in the 'periodic table' carbonitrides (Ti, Zr),

carbides (Nb, Ta) and finally borides (Fe, Cr) were produced. These trends also mirror electronegativity values,[14] as the elements showing lowest electronegativity formed nitrides and those with highest electronegativity formed borides. The apparently anomalous behaviour of Y may fit into a broader pattern if other elements from the low electronegativity region of the 'periodic table' were to be investigated.

In order to explain the formation of the refractory carbides, nitrides and borides it is necessary to consider the reaction conditions prevailing during the heating cycle. Up to 30 vol.% of the graphite furnace atmosphere has been found to consist of carbon monoxide and it is this which accounts for the formation of carbides in the reaction products, as the carburisation of metals is frequently carried out in such an atmosphere. The source of the carbon monoxide is most likely to be the reaction between the graphite elements and residual oxygen remaining after outgassing or that liberated from the oxides in the samples themselves. At the temperatures used in the experiments BN decomposes into B and N_2. The boron is free to react and this accounts for the formation of the borides found in the Fe- and Cr-containing samples. Nitride formation is due to reaction with the furnace atmosphere or with the nitrogen liberated from the decomposition of the BN, which would be in a reactive (nascent) state.

The oxynitride of Al which forms is generally well predicted by McCauley & Corbin's AlN–Al_2O_3 phase diagram,[15] which indicates that below 1920°C AlN should be in equilibrium with the non-stoichiometric spinel phase and above that temperature with an AlN polytypoid. However, the phase diagram indicates that the appropriate polytypoid is the 27R phase at 1950°C. While this was found to be so in the MgO–AlN and TiO_2–AlN systems, in the Cr_2O_3–AlN, Fe_2O_3–AlN and Nb_2O_5–AlN systems the 21R polytypoid was encountered in samples richest in reactant oxide at a temperature of 50°C below that given on the phase diagram. The possibility that the lowest formation temperature of the 21R AlN polytypoid might be about 1950°C in the AlN–Al_2O_3 system has been previously indicated by Sakai.[16] The reason for this apparent lowering of the formation temperature is not yet clear and it also remains to be seen whether the temperature threshold for the formation of the 27R AlN polytype is also reduced in these systems. In addition to the 27R and 21 polytypoids, a 33R AlN polytypoid was found in two systems, AlN–MgO and AlN–Fe_2O_3. Similarly the 16H AlN polytypoid was found in the 10AlN:1Cr_2O_3 sample. These phases have not been recorded in these systems before (cf. Ref. 5).

The nitride, carbide and boride phases have morphologies quite different from AlN or the oxynitride phases formed, making them easily detected using scanning electron microscopy. The morphology of the AlN polytypoids was found to be variable. In the AlN–MgO, AlN–TiO_2 and AlN–Cr_2O_3 systems these polytypoids were found to be needle-like, while in the AlN–Fe_2O_3 and AlN–Nb_2O_5 systems they were indistinguishable from the equiaxed matrix. In most previous reports of AlN and sialon polytypes, it has been noted that these crystals take a lath-like or needle-like form,[17–19] although Sakai[16] observed a plate-like morphology for 27R AlN polytypoid crystals formed in the AlN–Al_2O_3 system. It is well known that impurities can affect the growth morphology of a crystal although the way in which impurities influence morphology of the AlN polytypoids is not understood. However, as the foreign metal does not enter the structure in significant quantities it would appear that the crystal growth and resultant morphology is due to surface processes rather than bulk processes and these processes must be different in the case of Nb and Fe to the system where needle-like crystals form.

In the AlN–Y_2O_3 system the grain morphology was found to be dependent on the amount of Y_2O_3 present and the specimens heated at 1950°C were all different from one another. Similar effects were also noticed by Komeya & Inoue[2] who found that specimens of AlN–Y_2O_3 containing up to 25 wt% Y_2O_3 and heated at 1700°C or higher showed well-developed and randomly oriented fibrous texture, but with increasing Y_2O_3 content this changed to a granular structure. The fibrous crystals were identified as AlN and had a very positive effect on the observed flexural strength.

Although some aspects of these complex systems have been clarified more studies are needed before the compositions and structures of the unidentified phases are resolved and the role of the metal oxides in controlling the sintering behaviour, morphology and type of polytypoid phases formed has been clarified.

Acknowledgements

PJC is indebted to Sandvik Ltd and the SERC for financial support. All authors are grateful to Dr David Jack for his interest and encouragement during the course of this study and to Dr Björn

Ahrenius for most helpful discussions of the thermodynamics of the reactions investigated.

References

1. Virkar, A., Jackson, T. & Cutler, I. B., Thermodynamic and kinetic effects of oxygen removal on the thermal conductivity of aluminium nitride. *J. Amer. Ceram. Soc.*, **72** (1989) 2031–42.
2. Komeya, K. & Inoue, H., The influence of fibrous aluminium nitride on the strength of sintered AlN–Y_2O_3. *Trans. J. Brit. Ceram. Soc.*, **70** (1971) 107–13.
3. Yagi, T., Shinozaki, K., Mizutani, N., Kato, M. & Sawada, Y., Migration of grain boundary phases in AlN ceramics by heating in reduced atmospheres. *J. Ceram. Soc. Japan*, **97** (1989) 1372–8.
4. Komeya, K., Inoue, H. & Tsugi, A., The effect of various additives on sintering of aluminium nitride. *J. Ceram. Soc. Japan*, **89** (1981) 330–6.
5. Jack, K. H., Sialons and related nitrogen ceramics. *J. Mater. Sci.*, **11** (1976) 1135–58.
6. Weiss, J., Greil, P. & Gauckler, L. J., The system Al–Mg–O–N. *J. Amer. Ceram. Soc.*, **65** (1982) C68–C69.
7. Kuang, S. F., Huang, Z. K., Sun, W. Y. & Yen, T. S., Phase relationships in the system MgO–Si_3N_4–AlN. *J. Mater. Sci. Letters*, **9** (1990) 69–71.
8. Stoto, T., Doukham, J. C. & Mocellin, A., Analytical electron microscopy investigation of the AlN–ZrO_2 system: identification of a quaternary Zr–Al–O–N phase. *J. Amer. Ceram. Soc.*, **72** (1989) 1452–7.
9. Hagege, S., Ishida, Y. & Tanaka, S. I., TEM analysis of impurity induced microstructures in sintered aluminium nitride ceramics. *J. Ceram. Soc. Japan*, **96** (1988) 1119–26.
10. Troczynski, T. B. & Nicholson, P. S., The effect of additives on the pressureless sintering of aluminium nitride between 1500 and 1800°C. *J. Amer. Ceram. Soc.*, **72** (1989) 1488–91.
11. Brandt, B. G. & Nord, A. G., A set of crystallographic programs for an IBM 360/75 computer. *Chem. Commun. Univ. Stockholm*, No. 5 (1970).
12. JCPDS Powder Diffraction File, International Center for Diffraction Data, Swarthmore, PA, Card Numbers 38-1420, 32–1383, 1990.
13. JCPDS Powder Diffraction File, International Center for Diffraction Data, Swarthmore, PA, Card Numbers 35-0753, 35-0784, 1990.
14. Gordy, W. & Thomas, W. J. O. J., Electronegativities of the elements. *J. Chem. Phys.*, **24** (1956) 439–44.
15. McCauley, J. W. & Corbin, N. D., High temperature reactions and microstructures in the Al_2O_3–AlN system. In *Progress in Nitrogen Ceramics*, ed. F. W. Riley. Martinus Nijhoff, The Hague, 1983, pp. 111–18.
16. Sakai, T., Hot-pressing of the AlN–Al_2O_3 system. *Yogyo Kyokai-Shi*, **86** (1978) 125–30.
17. Van Tendeloo, G., Faber, K. T. & Thomas, G., Characterisation of AlN ceramics containing long-period polytypes. *J. Mater. Sci.*, **18** (1983) 525–32.
18. Krishnan, K. M., Rai, R. S., Thomas, G., Corbin, N. D. & McCauley, J. W., Characterisation of long-period polytypoid structures in the alumina–aluminium nitride system. *Mater. Res. Soc. Symp. Proc.*, **60** (1986) 211–18.
19. Clarke, D. R. & Shaw, T. M., Polytypism in magnesium sialon. *Mater. Sci. Res.*, **11** (1978) 589–96.